Global kinetic model: A case study on the *N*-oxidation of alkylpyridines

Jun Gao, Maria Papadaki *

Chemical Engineering, School of Process Environmental and Materials Engineering, University of Leeds, Leeds LS2 9JT, UK

Available online 21 October 2005

Abstract

The homogeneous catalytic *N*-oxidation of two picolines and two lutidines by hydrogen peroxide has been studied calorimetrically using a heat flow and power compensation SIMULAR reaction calorimeter. The objective of this work was to extend a previously developed kinetic model [J. Sempere, R. Nomen, J.L. Rodriguez, M. Papadaki, Modelling of the reaction of 2-methylpyridine using hydrogen peroxide and a complex metal catalyst, Chem. Eng. Process. 37 (1998) 33–46] for 2-methylpyridine to more reactions in the same family. The kinetic model is in good agreement with our experimental data on β-picoline. 3,5-Lutidine is in adequately good agreement with the model. However, the formation of two phases during the course of the reaction imposes the need for modifications to allow for mass transfer considerations. The *N*-oxidation of 2,6-lutidine is controlled by the addition or availability of hydrogen peroxide. A different reactor design is necessary for operation at the kinetic regime. High temperatures and catalyst concentrations enhance the selectivity towards *N*-oxidation of all alkylpyridines studied. The power evolution of all reactions has similar profiles thus indicating that similar kinetics are followed. The study of the *N*-oxidation of this family of compounds indicates that it is possible to design a process where hydrogen peroxide decomposition can be practically totally suppressed.
© 2005 Elsevier B.V. All rights reserved.

Keywords: α-Picoline; β-Picoline; 2,6-Lutidine; 3,5-Lutidine; Global kinetics; Isothermal calorimetry

1. Introduction

Exothermic chemical runaway reactions in batch and semi-batch processes can halt production and result in serious injuries, or even death, to plant operators. A thermal runaway begins when the heat produced by the reaction exceeds the heat removed by the cooling system. The thermal power (dq/dt) generated by a reaction is a function of the reaction rate:

$$\frac{\mathrm{d}q}{\mathrm{d}t} = (-\Delta H_r) \cdot r \cdot V \qquad (1)$$

where ΔH_r, r and V are the heat of reaction, the rate of reaction and volume of the reacting mixture, respectively.

In adiabatic operation, which is practically the case if an industrial reactor suffers a runaway, the rate of heat production increases exponentially until reaction completion. Under runaway conditions the reactor temperature can rise very high and very fast and cause initiation of thermally autocatalytic decomposition reactions as well. The reaction vessel may be at risk from over-pressurization due to violent reactor content boiling or rapid gas generation. One of the most serious hazards in chemical industry has its roots in runaway reactions [1]. Frequently, incidents involving thermal-runaways of chemical reactions are attributable to little or no research related with reaction chemistry/thermochemistry being done beforehand [2].

In order to evaluate thermal hazards of a reaction information is needed on the rates and the amounts of heat generated. For that purpose various techniques and tests have been developed to provide the necessary data. Isothermal calorimetry has been employed in the current study. Good quality calorimetrical data allow the accurate evaluation of the heat of reaction. Moreover, if they are combined with appropriate analytical measurements they can provide a firm ground for the development of "simple", directly applicable and reliable kinetic models. Such data were used in our previous work [3] for the development of a Langmuir type kinetic model for the *N*-oxidation of α-picoline (2-methylpyridine). However, for a model to be practical, it should accommodate as a wide range of reactions as possible. Such a development, can

* Corresponding author. Tel.: +44 113 343 2420; fax: +44 113 343 2420.
*E-mail address:* m.papadaki@leeds.ac.uk (M. Papadaki).

minimalise the number of necessary experiments for a specific process. In the current study we present results obtained from the calorimetric study of other members of the same family of reactions, notably the *N*-oxidation of β-picoline (3-methylpyridine), 2,6-lutidine and 3,5-lutidine.

2. Experimental and analytical

The reactions employed in this study are liquid, homogeneous, catalytic *N*-oxidations using hydrogen peroxide as the oxidant. Phosphotungstic acid is the catalyst used, which is totally or partially soluble in the employed liquids. The macroscopically occurring reactions under the conditions of the measurement are: (i) the *N*-oxidation of the employed alkylpyridine for the formation of the respective alkylpyridine-*N*-oxide and (ii) the competitive catalytic decomposition of hydrogen peroxide producing gaseous oxygen.

$$2\,H_2O_2 \rightarrow 2\,H_2O + O_2 \tag{ii}$$
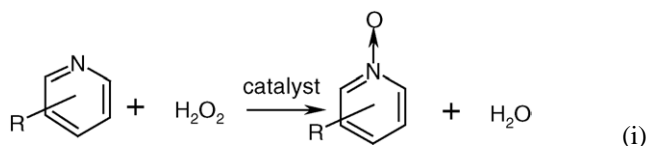
The following alkylpyridines were employed in the current study:

α-picoline

β–picoline

3, 5 lutidine and

2, 6 lutidine
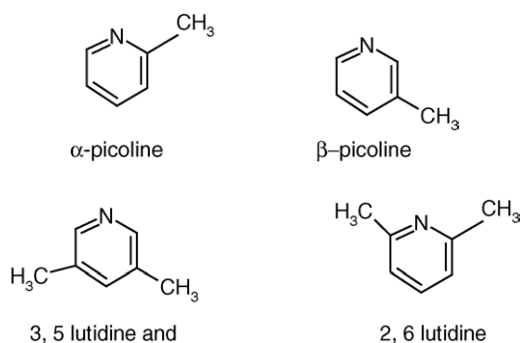
The equipment used to perform the measurements presented in this work was a SIMULAR reaction calorimeter, a sketch of which is shown in Fig. 1. The reactions have been performed isothermally at similar to industrial conditions. The alkylpyridine and the catalyst were added into the reactor (1) and the system was heated to the desired process temperature by means of thermal fluid circulating in the reactor jacket. An excess of hydrogen peroxide in the form of an aqueous solution was linearly added by means of pump (6) over the alkylpyridine/catalyst mixture for a period of approximately 3 h. Subsequently, reaction was left to completion. Throughout the course of reaction the system was agitated by means of agitator (4) and the produced by the hydrogen peroxide decomposition oxygen was continuously measured by an accurate MKS mass flowmeter.

The employed calorimeter is a fully computer-controlled unit. The temperatures of the reactor, oil entering and leaving the reactor, water entering and leaving the condenser, the ambient temperature, the indication of scales, pumping rate, agitator speed, oxygen mass flow-rate as well as a number of other optional quantities were continuously measured and registered with the computer. The instrument can operate as a *power compensation* and *heat flow calorimeter* and both modes have been employed in the current study. A comparison of the two methods is shown in our previous work [4].

The total thermal power, (dq_r/dt), produced by the reaction system can be obtained by the following energy balance over the reactor:

$$\frac{dq_r}{dt} = \frac{dq_{ac}}{dt} + \frac{dq_{dos}}{dt} - \frac{dq_c}{dt} - \frac{dq_{stir}}{dt} + \frac{dq_f}{dt} + \frac{dq_{loss}}{dt} + \frac{dq_{cond}}{dt} \tag{2}$$

where dq_{ac}/dt, dq_{dos}/dt, dq_c/dt, dq_{stir}/dt, dq_{loss}/dt, dq_{cond}/dt are terms of thermal power owing to accumulation, addition of mass in the reactor, calibration, stirring, losses and condenser duty, respectively. All quantities are either measured or calculated following methodologies presented for instance by Regenass [5] and Zaldivar et al. [6]. The methodology followed in the current work is shown in our previous articles [4,7,8].

The power (dq_2/dt), owing to the hydrogen peroxide decomposition, was calculated from relation (3). n Indicates number of moles of the substance identified by the suffix and ΔH_2 the heat of decomposition of hydrogen peroxide, previously measured [9] and found similar to the literature value, approximately equal to 100 kJ/mol of hydrogen peroxide.

$$\frac{dq_2}{dt} = -\Delta H_2 \cdot 2 \cdot \frac{dn_{Oxygen}}{dt} \tag{3}$$

The unreacted moles of hydrogen peroxide present in the reactor at time t can be calculated from a mass balane (Eq. (4)), where n indicates number of moles. The suffices identify the compound of reference. Suffix 0 has been used to indicate initial quantities and suffix t the moles present in the reactor at time t. n_{oxygen} corresponds to the total number of oxygen moles formed until time t.

$$n_{H_2O_2,t} = n_{H_2O_2 dosed,t} - (n_{alkylpyridine,0} - n_{alkylpyridine,t}) - 2 \cdot n_{oxygen} \tag{4}$$

The thermal power dq_1/dt, owing to the *N*-oxidation can be calculated via relation (5) and the moles of alkylpyridine present in the reactor at time t from Eq. (6).

$$\frac{dq_1}{dt} = \frac{dq_r}{dt} - \frac{dq_2}{dt} \tag{5}$$

$$n_{alkylpyridine,t} = n_{alkylpyridine,t_f}\left(1 - \frac{q_{1t}}{q_{1t_f}}\right) \tag{6}$$

where q_{1t} is the thermal power evolved by the *N*-oxidation reaction at time t. q_{1t_f} is the total thermal power evolved by

Fig. 1. Calorimeter schematic.
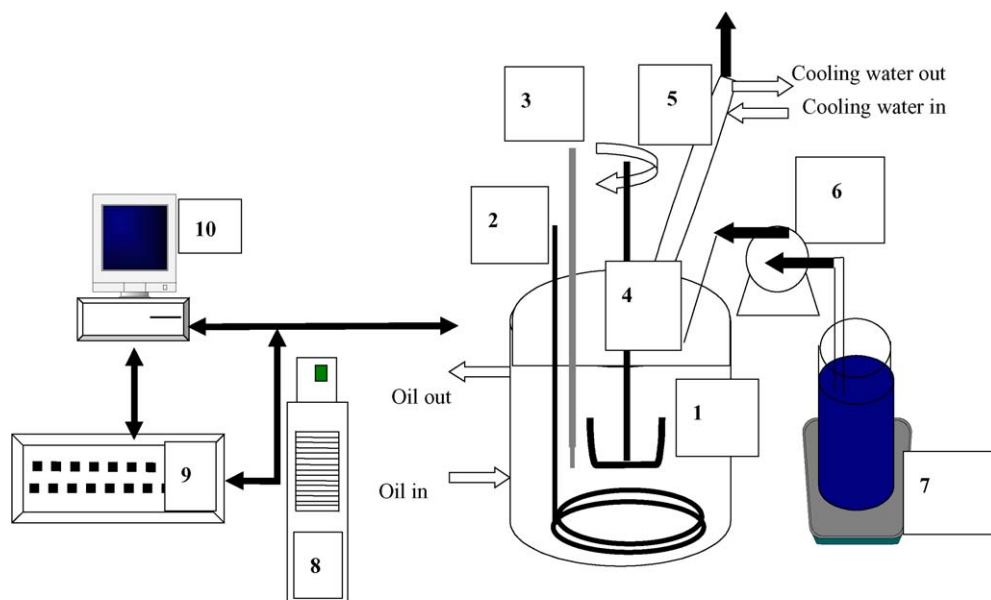
1	Reactor
2	Calibration heater (used for the evaluation of the effective heat transfer coefficient)
3	Platinum resistance thermometer
4	Agitator
5	Double pass condenser
6	Pump for reactant addition
7	Scales for holding the dosed reactant
8	Thermostatic bath
9	Control unit
10	Computer

all the alkylpyridine that has reacted at time t_f marking the end of the reaction.

The raw-materials used were β-picoline (FLUKA80230, 98%), 3,5-lutidine (ALDRICH L-420–6, 98%), 2,6-lutidine (ALDRICH 33610–6, 98%) and aqueous solution of hydrogen peroxide (FLUKA 95299, 35%).

Measurements were performed isothermally in the temperature range 85–100 °C, using different amounts of catalyst.

Samples were regularly taken, diluted, (0.1 g sample in 250 ml water) and their concentrations were measured by means of high performance liquid chromatography (HPLC) using a LaChrom L-7400 UV detector. Compounds were seperated using a 150 mm × 3.9 mm Symmetry Shield (RP8) column and the mobile phase was 80/20 H$_2$O/ACN. Concentration was measured using the UV detector at 254 nm. Mobile phase flow-rate was set at 1.0 ml min^{-1}, at a pressure of 2000 MPa.
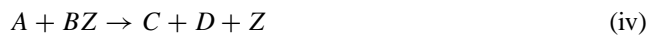
The calorimetrically obtained concentrations, which were in excellent agreement with the analytical measurements, were subsequently used in kinetic simulations. As previously said, the model of Sempere et al. [3], based on the α-picoline N-oxidation has been used for that purpose. The model consists of stoichiometric Eqs. (iii)–(viii) and equilibrium, mass balance and rate Eqs. (7)–(14). The model is based on the assumption of a fast, always in equilibrium, reaction between hydrogen peroxide and catalyst forming an intermediate. The intermediate subsequently reacts in a number of ways to form the final products. The model is quoted here for the reader's convenience.

$$B + Z \leftrightarrows BZ \tag{iii}$$

$$[BZ] = K_b \cdot [B] \cdot [Z] \tag{7}$$

$$\frac{Z_0}{V} = [Z] + [BZ] \tag{8}$$

$$[Z] = \frac{Z_0}{(1 + K_b \cdot [B])V} \tag{9}$$

$$A + BZ \rightarrow C + D + Z \tag{iv}$$

$$r_{1a} = \frac{K_b \cdot k_{1a} \cdot Z_0 \cdot [A] \cdot [B]}{(1 + K_b \cdot [B]) \cdot V} \tag{10}$$

$$A + B \rightarrow C + D \tag{v}$$

$$r_{2b} = k_{2b}[A] \cdot [B] \tag{11}$$

$$2\,BZ \rightarrow 2D + E + 2\,Z \tag{vi}$$

$$r_{2a} = \frac{K_b^2 \cdot k_{2a} \cdot Z_0^2 \cdot [B]^2}{(1 + K_b \cdot [B])^2 \cdot V^2} \tag{12}$$

$$B + BZ \rightarrow 2D + E + Z \tag{vii}$$

$$r_{2b} = \frac{K_b \cdot k_{2b} \cdot Z_0 \cdot [B]^2}{(1 + K_b \cdot [B]) \cdot V} \tag{13}$$

alkali induced decomposition (viii)
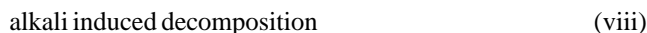
$$r_{2c} = K_{ab} \cdot k_{2c} \cdot [A][B]^2 \tag{14}$$

$$[B] = \frac{K_{ab} \cdot [B_{\text{apparent}}]}{(1 + K_{ab} \cdot [A])} \tag{15}$$

where the concentration of hydrogen peroxide, $[B]$, is calculated via the empirical relation (15), B_{apparent} the accumulated hydrogen peroxide, which has not decomposed or reacted to produce 2-methylpyridine-*N*-oxide. Other notation used: square brackets indicate concentration. *A–E* correspond to 2-methylpyridine, hydrogen peroxide, *N*-oxide, water and oxygen, respectively. k_{ij} are kinetic coefficients and K_j equilibrium coefficients. Suffix 1 is used to indicate constants related to the *N*-oxidation reaction and suffix 2 refers to the hydrogen peroxide decomposition. Suffices *a–c* indicate different paths via which reactions (i) and (ii) proceed. Reaction (viii) has not been specified; data are merely fitted to Eq. (14).

3. Results and discussion

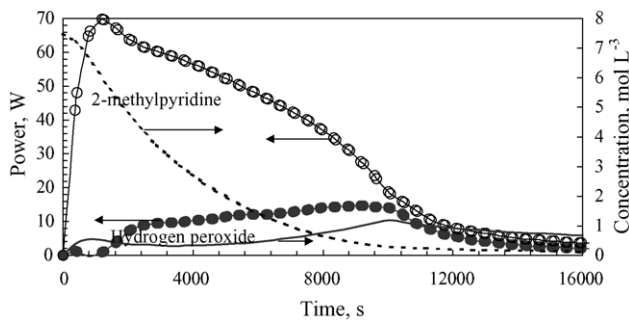Fig. 2 shows the thermal power generation and the calorimetrically obtained concentration profiles of a typ-

Fig. 2. Calorimetrically obtained thermal power and concentration of α-picoline (2-methylpyridine) and hydrogen peroxide. Lines have been used for concentration and markers for thermal power.
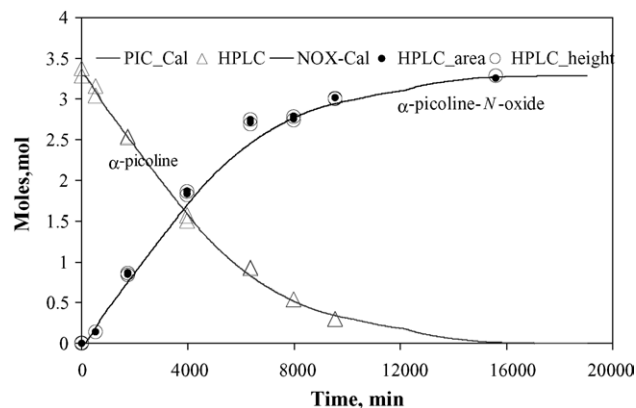

Fig. 3. Comparison of calorimetrically and analytically obtained concentration for 2-methylpyridine (α-picoline) and its *N*-oxide (α-picoline-*N*-oxide). Continuous lines correspond to calorimetric values and markers to the HPLC ones. Triangles have been used for α-picoline and circles for its *N*-oxide.

ical measurement performed in α-picoline. Fig. 3 shows the agreement between calorimetrically and analytically obtained concentrations of α-picoline and its *N*-oxide.

Fig. 4 shows the thermal power produced by the *N*-oxidation of α-picoline in three measurements performed under the same conditions but the amount of catalyst used. Other conditions: method of measurement, heat flow calorimetry; temperature, 85 °C; initial moles of α-picoline, 300 g; initial amount of water diluted into the mixture, 140 g; amount 35% aqueous solution of hydrogen peroxide added at constant rate in the reactor, 500 g. It can be seen, and it has been previously reported [7] that reduced amounts of catalyst favour the decomposition of hydrogen peroxide. Moreover, it is reported in the same work that the heat of alkylpyridines with water is not negligible. To reduce the influence of the thermal effects of mixing in those measurements, the alkylpyridine used is initially diluted with water.

Fig. 5 shows two measurements on β-picoline at 90 °C using different amounts of catalyst. Other conditions of measurement: method of measurement, power compensation; amount of β-picoline employed, 300 g in the measurement
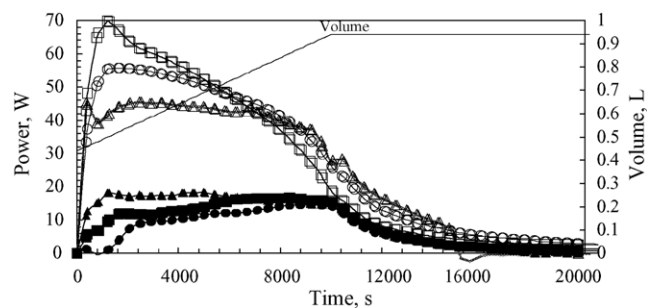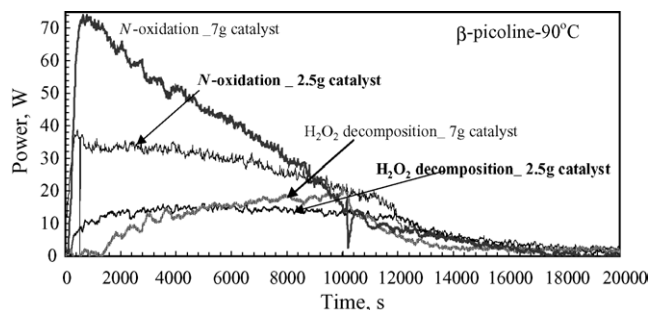

Fig. 4. Comparison of the power evolution due to *N*-oxidation and hydrogen peroxide decomposition in three measurements of α-picoline employing different amounts of catalyst. (□) *N*-oxidation 7 g catalyst, (●) decomposition 7 g of catalyst, (○) *N*-oxidation 3.5 g of catalyst, (■) decomposition 3.5 g of catalyst, (△) *N*-oxidation 2 g of catalyst and (▲) decomposition 2 g of catalyst.

Fig. 5. Comparison of the power evolution due to *N*-oxidation and hydrogen peroxide decomposition in two measurements of β-picoline employing different amounts of catalyst, at 90 °C.

Fig. 7. Comparison of the power evolution due to *N*-oxidation and hydrogen peroxide decomposition in two measurements of 2,6-lutidine employing different amounts of catalyst, at 90 °C.

where the highest amount of catalyst was used, 200 g in the other; initial amount of water used 200 and 300 g, respectively; amount of 35% aqueous solution of hydrogen peroxide added at constant rate in the reactor, 500 g.

Fig. 6 shows two measurements on β-picoline at 85 and 90 °C using different amounts of catalyst. Other conditions of measurement: method of measurement, power compensation; amount of β-picoline employed, 200 g in the measurement; initial amount of water used in both measurements, 300 g; amount of 35% aqueous solution of hydrogen peroxide added at constant rate in the reactor, 500 g.

As can be seen in Figs. 5 and 6 the behaviour of β-picoline is very similar to that of α-picoline, reported in our previous work [7]. Reduction of the employed amount of catalyst results in a significant reduction of the *N*-oxidation speed with a simultaneous acceleration of the decomposition reaction. Temperature has a similar effect in both substances. Higher temperatures favour the *N*-oxidation. Fig. 7 shows two measurements employing 2,6-lutidine. Other conditions: temperature, 90 °C; method of measurement, power compensation; amount of 2,6-lutidine employed in both measurements, 300 g; initial amount of water used, 200 g in the measurement with the lowest amount of catalyst and 150 in the other; amount of 35% aqueous solution of hydrogen peroxide added at constant rate in the reactor, 520 g in the measurement
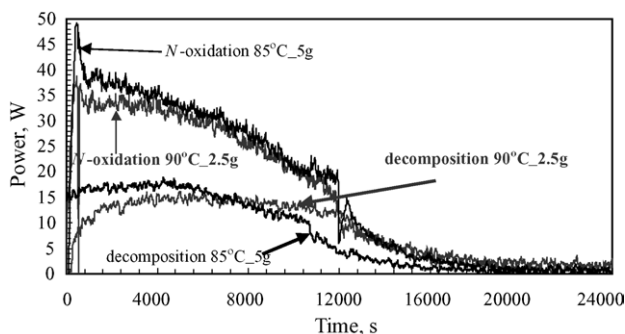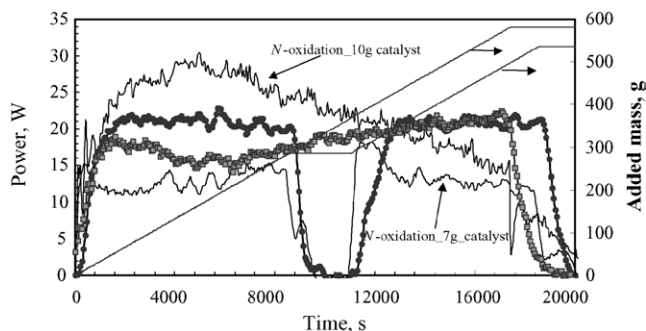
employing 10 g of catalyst and 580 g in the measurement employing 7 g of catalyst. In the measurement employing the smallest amount of catalyst dosing was temporarily interrupted. Both reactions were terminated, simultaneously with the interruption of dosing. Grey colour has been used for the measurement with 10 g of catalyst and black for the measurement with 7 g of catalyst. Closed markers are used for the decomposition and lines for the *N*-oxidation. It can be seen in this graph the importance that the catalyst concentration exerts on the relative rates of the two reactions. In the measurement employing the lowest amount of catalyst most hydrogen peroxide is consumed by the decomposition. In the measurement employing 50% more catalyst the *N*-oxidation predominates until its concentration is substantially reduced.

Fig. 8 shows a measurement performed with 3,5-lutidine using 7 g of catalyst. Other conditions: temperature, 90 °C; method of measurement, power compensation; amount of 3,5-lutidine employed in both measurements, 300 g; initial amount of water used, 200 g; amount of 35% aqueous solution of hydrogen peroxide added at constant rate in the reactor, 420 g. It can be seen in Fig. 8 that hydrogen peroxide decomposition is not as dramatic as in the case of 2,6-lutidine. Its rate of decomposition follows the same profile as in all other compounds considered. On the other hand, the rate profile of the *N*-oxidation is quite dissimilar to the ones obtained by the picolines. This was attributed to the fact that initially the mixture was not homogeneous. In the range of temperatures

Fig. 6. Comparison of the power evolution due to *N*-oxidation and hydrogen peroxide decomposition in two measurements of β-picoline employing different amounts of catalyst, at 85 and 90 °C.
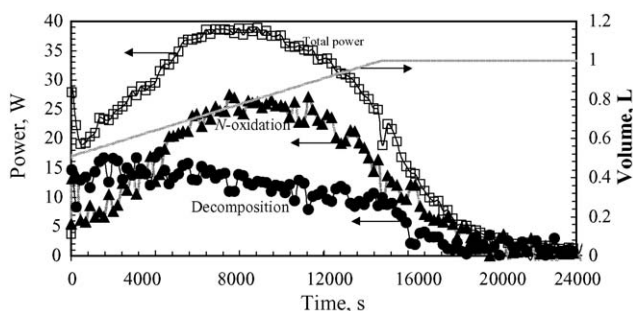

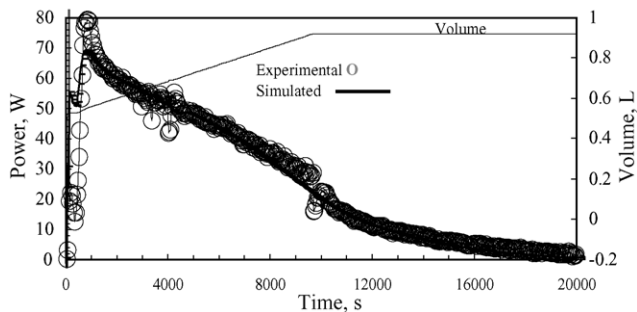Fig. 8. Power evolution during the *N*-oxidation of 3,5-lutidine at 90 °C, using 7 g of catalyst.

Fig. 9. Experimental and simulated thermal power for the *N*-oxidation of β-picoline at 85 °C and 10 g of catalyst, employing the aforementioned model.

Fig. 11. Hydrogen peroxide decomposition during the *N*-oxidation of 3,5-lutidine. Comparison of experimental with simulated values.

employed in the current study, the solubility of 3,5-lutidine in water is very small in a quite extensive range of compositions [10]. However, at temperatures higher than approximately 200 °C complete miscibility is possible for any concentration. This may suggest that operation at a higher pressure (that will allow higher temperatures for the reaction) could resolve that problem. Nevertheless, in the presence of catalyst, hydrogen peroxide and *N*-oxide, which affect the pH of the solution, the phase diagrams are expected (supported by recent experimental evidence) to be different. Otherwise, the behaviour of 3,5-lutidine was closer to the one of picolines than that of 2,6-lutidine.

The kinetic model cited above, which was extracted from the thermal study of α-picoline has been used to simulate the rates of the *N*-oxidation of β-picoline and the accompanying hydrogen peroxide decomposition of β-picoline. Comparisons showed that the model of the *N*-oxidation is in good agreement with our data as Figs. 9–11 demonstrate. Fig. 9 shows the agreement between the simulated and experimental results for a measurement in β-picoline at 90 °C employing 10 g of catalyst. Fig. 10 shows the same comparison for the parallel hydrogen peroxide decomposition under the same conditions. The initial part of this measurement cannot be simulated as the reaction is controlled by dosing (shown on
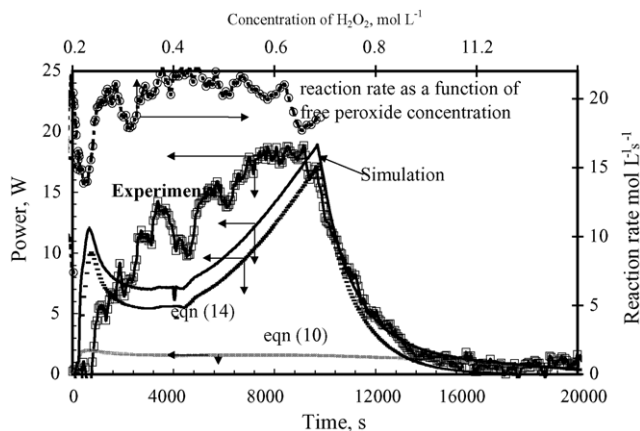
the secondary axes), or the availability of unreacted hydrogen peroxide which has been obtained via the empirical relation (15).

Fig. 11 shows the comparison of the simulated with the experimental results of the unwanted hydrogen peroxide decomposition, taking place during the *N*-oxidation of 3,5-lutidine, for the measurement shown on Fig. 8.

It is worth mentioning that the simulation of the measurements, shown in Fig. 9 practically correspond to the catalytic path of the *N*-oxidation. The contribution of the uncatalysed *N*-oxidation which, as mentioned in our previous work [7], was not observed when the reaction was attempted in the absence of catalyst, was insignificant. However, the hydrogen peroxide decomposition shown in Fig. 10 proceeds almost exclusively via the "alkali-induced" decomposition path, which again, as mentioned in Papadaki et al. [7], was not observed when the reaction of decomposition was attempted in the absence of catalyst. On the other hand, the hydrogen peroxide decomposition shown in Fig. 11, which accompanies the 3,5-lutidine *N*-oxidation, was modelled using exclusively the catalytic path, thus indicating, that in the case of phase separation the catalyst remains in the aqueous phase and accelerates the decomposition. This was also indicated from the comparison of the hydrogen peroxide concentrations in one phase and two-phase systems. Although in homogeneous mixtures the concentration of hydrogen peroxide rises after a substantial reduction of the alkylpyridine concentration this was not observed in the case of 3,5-lutidine, where an organic and an aqueous phase exist. When one phase mixture is used, the catalyst favours the *N*-oxidation.

The above results show that the equations of the model can simulate well the rates of other alkylpyridines. However, although the assumption of the formation of the intermediate between hydrogen peroxide and catalyst is well documented in literature [11] thus rendering the assumptions of the catalytic paths plausible, the uncatalysed *N*-oxidation and the "alkali-induced" decomposition paths represent the data adequately well but, they remain empirical rate equations and further research is needed in order to be replaced by catalytic paths. Further experiments are also necessary for the implementation of the methodology described in our previous

Fig. 10. Experimental and simulated thermal power for the hydrogen peroxide decomposition of β-picoline at 85 °C and 10 g of catalyst, employing the aforementioned model.
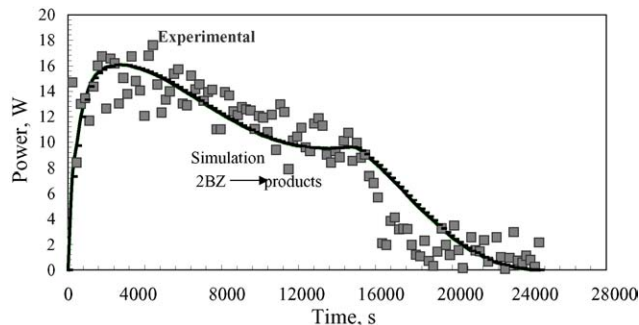
work [12] in regard with the accurate evaluation of rate coefficients. This objective has not been completed yet because at the concentrations and temperatures suggested the catalyst comes out of solution thus altering the heat-transfer characteristics of the mixture.

4. Conclusions

In the present article we present new calorimetric measurements on the *N*-oxidation of β-picoline, 3,5-lutidine and 2,6-lutidine. It was found that in all cases the selectivity of the *N*-oxidation is greatly enhanced in the presence of high catalyst concentrations. Also, temperature favours the *N*-oxidation reaction for all substances studied. Calorimetrically and analytically obtained concentration profiles are in good agreement. Our previous [3] kinetic model is in good agreement with our experimental data on β-picoline. In the presence of substantial amounts of catalyst, the *N*-oxidation proceeds catalytically. The so-called "alkali-induced" decomposition of hydrogen peroxide needs further investigation. The kinetic study of the system reveals that the process can be optimised so that more efficient reactor designs (higher temperatures, pressures and catalyst concentrations), that will allow suppression of the decomposition reaction can be enabled. Significant suppression of hydrogen peroxide decomposition can be achieved whilst the re-use of catalyst is also possible.

Acknowledgement

References

[1] Euroabstracts [Accesed 10-2-2004]. The Dangers of Over-Reacting [Online]. Available from: ⟨http://www.cordis.lu/euroabstracts/en/august98/trans1.htm⟩.

[2] J.A. Barton, P.F. Nolan, Incidents in the Chemical Industry due to Thermal-Runaway Chemical Reactions. IChemE Symposium Series No. 115 (1989) 3–13.

[3] J. Sempere, R. Nomen, J.L. Rodriguez, M. Papadaki, Modelling of the reaction of 2-methylpyridine using hydrogen peroxide and a complex metal catalyst, Chem. Eng. Process. 37 (1998) 33–46.

[4] J. Gao, M. Papadaki, *N*-oxidation of picolines and lutidines kinetic studies, in: CDRom Proccedings of the 4th European Thermal Sciences Conference 2004, Birmingham, UK, March 29–31, 2004.

[5] W. Regenass, Thermoanalytische methoden in der chemischen verfahrensentwicklung, Thermochim. Acta 20 (1997) 65–79.

[6] J.M. Zaldivar, H. Hernandez, C. Barcons, Development of mathematical model and a simulator for the analysis and optimisation of batch reactors: experimental model characterization using a reaction calorimeter, Thermochim. Acta 289 (1996) 267–302.

[7] M. Papadaki, V. Stoikou, D. Mantzavinos, J.L. Rodriguez-Miranda, Towards improved reaction runaway studies: kinetics of the *N*-oxidation of 2-methylpyridine using heat-flow calorimetry, Process Saf. Environ. Prot. 80 (2002) 186–196.

[8] M. Papadaki, H.P. Nawada, Towards improved reaction runaway assessment methods I. Simple calorimetric method of evaluation of heat transfer coefficient and reactor thermal mass, J. Chem. Reactor Eng. 1 (2003), article A40.

[9] M. Papadaki, Use of reaction calorimetry in thermal risk assessment studies and safe design of batch reactions that can lead to a runaway: application on hydrogen peroxide, Top. Catal. 29 (3) (2004) 207–214.

[10] H. Stephen, T. Stephen (Eds.), Solubilities of Inorganic and Organic Compounds, vol. 1, Binary Systems, Part 2, Pergamon Press, Oxford, 1963, p. 1487.

[11] B. Viswanathan, S. Sivasanker, A.V. Ramaswamy, Catalysis Principles and Applications, Narosa Publishing House, New Delhi, 2002, pp. 84–205.

[12] M. Papadaki, R.J. Emery, E. Serra, R. Nomen, J. Sempere, Sensitivity analysis of the 2-methylpyridine *N*-oxidation kinetic model, Green Chem. 4 (2002) 199–205.